Identification of the active compounds and their mechanisms of medicinal and edible Heigen based on UHPLC-Q-Exactive Orbitrap MS and network pharmacology

Qian ZHAO[1] (iD), Rong DING[1], Si Li[1], Chenghui WANG[2], Rui GU[2*]

Abstract

Heigen is the root and rhizomes of *Duhaldea Nervosa* Anderberg., a traditional medicine food homology herb used to treat rheumatoid arthritis in China,but the potential active components and the underlying mechanism have not been clarified. In this study, the chemical compounds and the components absorbed into the blood from Heigen were assessed using ultra-high performance liquid chromatography coupled with quadrupole Orbitrap high-resolution mass spectrometry. 72 chemical constituents were identified in Heigen, 13 blood prototypical constituents, and 9 metabolites were found in serum samples after intragastric administration of Heigen extracts to rats. Then, using network pharmacology and molecule docking, 10 compounds were assumed to be potentially key active compounds against RA, which may be via the multi-component, multi-target and multi-pathway interaction mechanism of Heigen in the treatment of RA, and also provides a pharmacological basis for the treatment of RA.

Keywords: *Duhaldea nervosa*; UHPLC-Q-Orbitrap HRMS; network pharmacology; serum pharmacochemistry.

Practical Application: The exploration of Heigen gives essential information for consumers and researchers to understand the chemical composition and bioactivities of Duhaldea nervosa, laying the foundation for the development and utilization of new resource food.

1 Introduction

Rheumatoid arthritis (RA) is an inflammatory disease that causes persistent synovial inflammation, edema, progressive bone erosion, and joint destruction, which is always accompanied by joint swelling and tenderness, influencing the mental life and life expectancy of patients (Alamgeer et al., 2020), it affects around 1% of the world's population and disproportionately affects women (Smolen et al., 2016). Unfortunately, the pathogenesis of RA has not been fully illustrated, which poses a major challenge to the treatment of RA. At present, nonsteroidal anti-inflammatory drugs (NSAIDs) (Bindu et al., 2020) and disease-modifying anti-rheumatic drugs (DMARDs) (Fonseca Peixoto et al., 2022) are common treatments for RA. However, traditional NSAIDs and DMARDs have significant gastrointestinal, hepatic, and renal toxicity (Min et al., 2022), glucocorticoids can cause side effects such as osteoporosis, hypertension, and hyperglycemia, while biologics can cause autoimmune syndromes (Li et al., 2022). The discovery of safer, efficacious formulations is critical for defeating RA disorders.

In recent years, natural plant extracts and compounds (NPECs) have been shown in preclinical tests to give considerable alleviation in rheumatoid arthritis, which displays the capability that more effective and less adverse reactions, especially considering the multi-target effect of these natural products (Dias et al., 2021). It is obvious that natural compounds derived from traditional herbal treatments are valuable sources of novel medication development. Heigen is the root and rhizomes of *Duhaldea nervosa* (Wallich ex Candolle) Anderberg (Figure 1), which is a valuable traditional medicine that is accustomed to treating rheumatoid arthritis, joint pain, and chronic gastritis. Besides, it is a medicinal and edible homology resource (Cheng et al., 2023). In the previous ethnobotanical surveys, we found that is quite common in local use, it is usually cooked into chicken soup to strengthen the body and prevent diseases, which is a widely used traditional tonic and edible immune modulating herb. Heigen can be used as a "medicine-food homology" herb for dietary supplements, and creating functional foods is a treatment avenue that can be used at different stages of the disease. In the future, the discovery of specific bioactive compounds in Heigen offers the possibility to serve as sources of functional food ingredients. However, the active ingredients of Heigen and their underlying mechanisms are not clarified.

UHPLC-Q-Exactive Orbitrap MS is an efficiency and sensitivity technique to detect and identify chemical components or biological sample (Li et al., 2020), it can rapidly identify known metabolites by ccomparing experimental spectral data with databases (Ghane et al., 2022). Network pharmacology is an emerging research approach combined with pharmacology, bioinformatics, and network biology (Lin et al., 2022). The compound-target-pathway networks can be predicted the biologically active ingredients and elaborate the compound mechanism of action (Wang et al., 2021). Today, network pharmacology comprehensively and systematically reveals the active ingredients (Jian et al., 2022) and potential mechanisms of action of TCM preparations by integrating multiple networks

Figure 1. Heigen: the roots and rhizomes of *Duhaldea nervosa* (Wallich ex Candolle) Anderberg.

connecting chemical substances, targets, diseases, and signaling pathways (Lee et al., 2019).

In this study, medicinal serum chemistry and network pharmacology methods were used to reveal the possible active components and mechanism of action of Heigen.

2 Materials and methods

2.1 Materials

High-performance liquid chromatography (HPLC)-grade acetonitrile and formic acid were purchased from Fisher (Thermo Fisher Scientific, MO, USA). Analytical-grade methanol was purchased from Chron Chemicals Co, Ltd. (Chengdu, China). Deionized water was p produced by Wahaha Group Co, Ltd. (Hangzhou, China). All standard compounds used in this study (Isochlorogenic acid A, Isochlorogenic acid B, Isochlorogenic acid C, Chlorogenic acid, Thymol) with a purity>98% were purchased from RuiFenSi Biotechnology Co, Ltd (Chengdu, China).

The batch of *Duhaldea Nervosa* Anderberg was collected in Yanbian county (Panzhihua, China) and authenticated by Professor Rui Gu (School of the Chengdu University of Traditional Chinese Medicine).

2.2 Preparation of Heigen extract

The samples which powered and passed through a 40-mesh sieve were accurately weighted (200 g), to be extracted by heating reflux with 1200 mL water for 1.5h, repeating 3 times, drying to 1 g/mL, for animal experiments.

Take 1 g of Heigen sample powder (<40), weigh it, and add 50 mL of 75% methanol-water (v/v). After heat reflux for 1h, the extract was cooled to room temperature, and taking 1 ml of the supernatant filteredlter through a 0.22 µm filter, for UHPLC-Q-Orbitrap HRMS analysis.

2.3 Preparation of serum samples

Grade SPF Male Sprague-Dawley (SD) rats(180g±20g) were purchased from Chengdu Dossy Experimental Animals

Co, Ltd (Chengdu, China. Rats were bred in the Faculty of Pharmacy of the Chengdu University of Traditional Chinese Medicine (Certificate NO. SYXK(Chuan)2020-124). 12 SD rats were accidentally divided into a blank group and an experiment group. The experimental group received 15 g/kg Heigen extract, and the blank group received the same amount of normal saline.

After administration, 0.5 mL blood samples were collected from the orbital venous plexus into centrifuge tubes at fixed time points (0.5, 1 h, 1.5 h, 2 h, 2.5 h, 3 h, 4 h). After centrifugation at 12000 rpm for 10 minutes, the supernatant was separated to obtain drug-containing serum. The drug-containing serum of the experimental group was mixed to 600 µL at7-time points, 3 mL of acetonitrile was added, shaken for 2 min, and centrifuged at 12000 rpm for 10 min. The supernatant was dried under nitrogen flow, and the processing steps were the same as those of the blank group. The dried residue was dissolved in 200 µl acetonitrile and filtered through a 0.22 µm Millipore filter before analysis.

2.4 UHPLC-Q-Orbitrap HRMS analysis condition

Both the Heigen extract and serum samples were analyzed using Vanquish UHPLC system (Thermo Fisher Scientific, Bremen, Germany) equipped with Q Exactive quadrupole-electrostatic field orbitrap high-resolution mass spectrometer. Chromatographic separation was performed on a: Thermo Scientific Accucore C18 column (3.0×100 mm, 2.6 µm, Thermo). The column temperature was set at 30 °C and the flow rate was 0.3 mL/min. The mobile phase consisted of deionized water with 0.1% formic acid (A) and acetonitrile with 0.1% formic acid (B). The gradient elution program was as follows: 0-3 min, 10%-25% B; 3-10 min, 25% -36% B;10-13 min, 36%-63% B;13-23 min, 63%-69% B; 23%-24 min, 69%-81%; 24-37 min, 81%-88% B; 37-40 min, 88-90% B.40-50 min, 90-10%.

Mass spectrometry was performed in positive and negative ion modes. The auxiliary gas and protective gas are both nitrogens, and the flow rates are 10 L/min and 35 L/min, respectively. The positive and negative mode ion spray voltages were 3 kV(+) and 3.0 kV(-), respectively. The temperature of the ion source and the heating temperature of the auxiliary gasise both 320 °C. Fragmentation voltage set to 20, 40, 60 eV, mass ratio scanned in m/z 100-1500.

Data acquisition and processing were performed using Xcalibur 2.1 (Thermo Fisher Scientific, San Jose, CA, USA), and analyzed by Compound Discoverer software (Thermo Fisher Scientific, San Jose, CA, USA).

2.5 network pharmacology study

Target related to bioactive ingredients of Heigen

Targets related to bioactive ingredients in Heigen were based on the analysis of the components in the serum of rats that were administered Heigen exacted, and the SDF files were downloaded from the PubChem database (Lin at al., 2022). Using Swiss Target Prediction to get an accurate prediction of the potential targets. the organism set to "Homo sapiens" and the probability ≥ 0.1, moreover, through UniProt Knowledgebase (UniProtKB, Yin et al., 2022) to standardize the gene names.

RA-Related targets and common targets between Heigen and RA

Using databases including DisGeNET (Zhao et al., 2021), GeneCards, DrugBank, OMIM (Hu et al., 2022), TTD (Liu et al., 2021) to search for genes related to RA by the keywords "rheumatoid arthritis". Potential Bioactive Target Genes from Absorbed Components for RA by using the Venn online platform (Yin et al., 2022).

Construction of the protein-protein interaction network

The potential bioactive target genes were imported into the STRING database (Yin et al., 2022) to construct the relationship of the protein-protein interaction (PPI) network, analyzed by Cytoscape 3.9.0.

Gene Ontology and KEGG Pathway Enrichment Analysis

Gene Ontology (GO) and Kyoto Encyclopedia of Genomes (KEGG) pathway analyzes were performed using the Metscape database (Zhang et al., 2022) with a screening criterion of $p < 0.1$, and input the analysis results into the Bioinformatics platform to visualize (Zhang et al., 2022).

Component–Target–Pathway Network

Use active components, common targets, and signaling pathways as nodes and create appropriate relationships in Excel.

Using Cytoscape 3.9.0 to build a "Component–Target–Pathway" network of Heigen for the treatment of RA.

2.6 Molecular docking

The structure of the receptor protein is from the RCSB Protein Data Bank database (Yang et al., 2022), and the removal of water, protonatiand, energy minimization by PyMOL. Molecular docking was performed by AutoDock Vina.

3 Results

3.1 composition analysis of HeiGen

A total of 72 compounds were identified by UHPLC-Q-Orbitrap HRMS in the positive and negative ion mode, and data acquisition and processing were performed using Xcalibur 2.1 (Thermo Fisher Scientific, San Jose, CA, USA), and analyzed by Compound Discoverer software (Thermo Fisher Scientific, San Jose, CA, USA). The results are as follows (Table 1).

3.2 composition analysis of rat serum

The total ion chromatograms of mouse serum samples administered in positive and negative ion modes are shown in Figure 2 and result shown in Table 2. Based on accurate measurements of mass, retention time, fragmentation behavior, reference standards, and related literature, a total of 13 representative
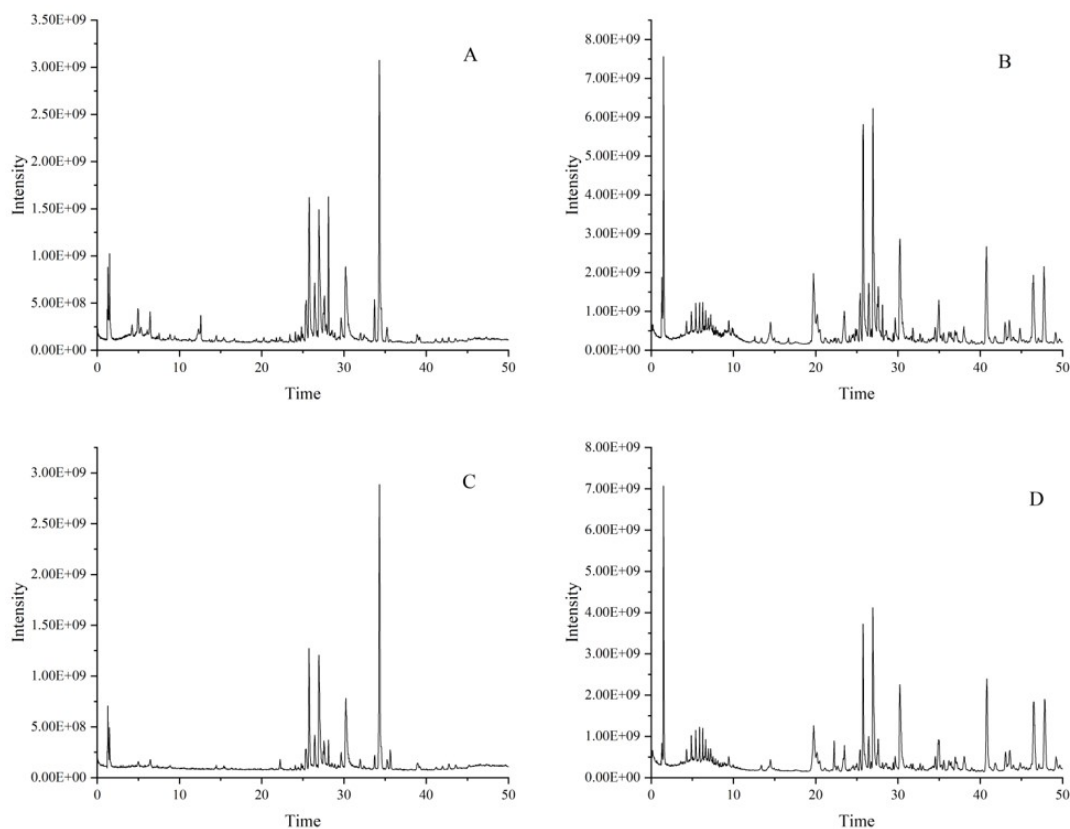

Figure 2. The UHPLC chromatographic of serum spectra in-vivo compared with the blank control group; A, B: Serum sample collected after oral administration of Heigen; C, D: Blank serum. These samples were detected in positive ion (right) and negative ion (left) modes in the UPLC-Q-Orbitrap HRMS.

Table 1. UHPLC-Q-Orbitrap HRMS data of the identified component of Heigen extract.

NO.	tR(min)	Identification	Formula	Theoretical Mass m/z	Experimental Mass m/z	Ion mode	Error(ppm)	MS/MS Fragment Ions
1	1.311	Quinic acid	$C_7H_{12}O_6$	192.06344	191.06339	-	0.29	173.04541,127.03965,111.00825,93.03391
2	1.317	Trigonelline	$C_7H_7NO_2$	137.04808	138.05550	+	2.90	94.0659
3	1.367	DL-Malic acid	$C_4H_6O_5$	134.02112	134.02152	-	-3.04	115.00318,189.01858,71.01306
4	1.500	Succinic acid	$C_6H_6O_4$	118.02617	118.02661	-	-3.68	99.00818,71.01290
5	1.701	hydroxymethylfurfural	$C_6H_6O_3$	126.03222	126.03169	+	4.18	109.02909,71.05002,53.03947
6	1.996	Gallic acid	$C_7H_6O_5$	170.02144	169.01416	-	-0.47	125.02396
7	2.627	Vanillic acid	$C_8H_8O_4$	168.04231	168.04226	-	0.31	152.01131,123.04471,95.01313
8	2.766	3-Hydroxymandelic acid	$C_8H_8O_4$	168.04231	168.04226	-	0.31	149.02426,123.04471
9	3.053	Protocatechuic acid-4-glucoside	$C_{13}H_{16}O_9$	316.08052	316.07943	-	3.44	153.01915,109.02897,108.02114
10	3.179	Protocatechuic acid	$C_7H_6O_4$	154.02652	154.02661	-	-0.59	109.02895
11	3.639	coniferyl aldehyde	$C_{10}H_{10}O_3$	178.06372	178.06299	+	4.09	161.06026,149.06030,103.05499
12	3.823	CQA-3'-glycoside	$C_{22}H_{28}O_{14}$	516.15022	516.14924	-	1.90	341.08755,353.11353,323.07819,191.05629,161.02429
13	4.256	Scopolin	$C_{16}H_{18}O_9$	354.09622	345.09508	-	3.23	191.05623
14	4.310	CA-hexoside	$C_{15}H_{17}O_9$	342.09639	342.13280	-	3.82	179.03502,135.04480
15	4.351	citric acid	$C_6H_8O_7$	192.02717	191.27000	-	1.04	85.02879,87.00807,111.00826
16	4.379	Sinapinic acid	$C_{11}H_{12}O_5$	224.06924	224.06847	+	3.43	147.04456,132.02094
17	4.635	Cryptochlorogenic acid	$C_{16}H_{18}O_9$	354.09613	354.09508	-	2.93	191.05623,179.03493,173.04547,135.04482
18	4.688	3-Feruloylquinic acid	$C_{17}H_{19}O_9$	368.11205	368.11073	-	3.59	193.05074
19	5.057	Pimelic acid	$C_7H_{12}O_4$	160.07344	160.07356	-	-0.75	115.07593,97.06523
20	5.091	Caffeic acid	$C_9H_8O_4$	180.04237	180.04226	-	0.63	135.04457,117.03414,107.04974
21	5.399	Epicatechin	$C_{15}H_{14}O_6$	290.08026	290.07904	-	4.20	245.08272,203.07173,123.04475,109.02896
22	5.408	Catechin	$C_{15}H_{14}O_6$	290.08026	290.07904	-	4.20	245.08272,161.03987,137.02423,109.02896
23	5.745	2,4-Dihydroxybenzoic acid	$C_7H_6O_4$	154.02661	154.02661	-	-0.62	135.00842,109.02895
24	5.973	5-Feruloylquinic acid	$C_{17}H_{19}O_9$	368.11198	368.11073	-	3.48	191.05624
25	6.518	Sedanolide	$C_{12}H_{18}O_2$	194.13126	194.13068	+	2.98	149.13306,93.07068,81.07072
26	7.149	isoquercitrin	$C_{21}H_{20}O_{12}$	464.09709	464.09548	-	3.48	300.02847,271.02579,255.03061,151.00346,107.01323
27	7.156	Quercetin	$C_{15}H_{10}O_7$	302.04357	302.04265	+	3.02	257.04504,229.05029,165.01872,153.01862,137.02380
28	7.209	Ferulic acid	$C_{10}H_{10}O_4$	194.05856	194.05791	+	3.34	177.05521,145.02892,117.03412,89.03938
29	7.628	Fraxetin	$C_{10}H_8O_5$	208.07436	208.07356	+	3.84	181.08638,163.11223,149.06024,121.06545
30	7.737	Chlorogenic acid	$C_{16}H_{18}O_9$	354.09612	354.09508	+	2.25	163.03938,135.04446
31	7.743	Isochlorogenic acid B	$C_{25}H_{24}O_{12}$	516.12810	516.12678	-	2.57	173.04550,179.03503,153.08896
32	8.034	Isochlorogenic acid A	$C_{25}H_{24}O_{12}$	516.12795	516.12678	-	2.28	191.05624,353.08902,179.03511,161.02434
33	8.036	Neochlorogenic acid	$C_{16}H_{18}O_9$	354.09614	354.09508	-	2.06	191.05623,179.03497,135.04482
34	8.414	Quercetin-3β-D-glucoside	$C_{21}H_{20}O_{12}$	464.09698	464.10425	-	3.25	301.03638,178.99867
35	8.449	Isoferulic acid	$C_{10}H_{10}O_4$	194.05872	194.05791	+	4.17	177.05521,145.02896,123.04463
36	8.857	Isochlorogenic acid C	$C_{25}H_{24}O_{12}$	516.12798	516.12678	-	2.33	173.04552,179.03505,353.08905,93.03395
37	8.981	3-FQA-hexoside	$C_{23}H_{29}O_{14}$	530.14420	530.14243	-	3.34	367.10458,193.04546,173.04546
38	8.984	4-FQA-hexoside	$C_{23}H_{29}O_{14}$	530.14420	530.14243	-	3.34	367.10437,193.05077,179.03494
39	9.239	3-caffeoyl-4-feruloyquinic acid	$C_{26}H_{25}O_{12}$	530.14419	530.14243	-	3.33	367.10458,335.07816,193.05080,173.04546
40	9.239	4-caffeoyl-5-feruloyquinic acid	$C_{26}H_{25}O_{12}$	530.14423	530.14243	-	3.40	367.10483,353.08903,173.04552,179.03503,191.05629,135.04483
41	9.253	CQA-pentoside	$C_{22}H_{27}O_{13}$	500.13363	500.13186	-	3.53	337.09402,179.03506,191.05627
42	9.447	Isferulic acid	$C_{10}H_{10}O_4$	194.05819	193.05092	-	1.45	178.02724,134.03700
43	9.503	4-Hydroxybenzoic acid	$C_7H_6O_3$	138.03145	138.03169	-	-1.80	93.03393
44	9.503	Salicylic acid	$C_7H_6O_3$	138.03149	139.03169	-	-1.46	93.03389
45	9.627	1,3- Dicaffeoylquinic acid	$C_{25}H_{24}O_{12}$	516.12810	516.18429	-	4.11	191.05626,173.04553,179.03506
46	10.059	4-Feruloylquinic acid	$C_{17}H_{19}O_9$	368.11149	368.11073	-	2.07	173.04553
47	10.081	5-FQA-hexoside	$C_{23}H_{29}O_{14}$	530.14423	530.14243	-	3.34	367.10321,191.05623,173.04555
48	11.189	Luteolin	$C_{15}H_{10}O_6$	286.04901	286.04774	+	4.46	217.05087,133.02911,151.00310,107.01334
49	13.106	DL-Mandelic acid	$C_8H_8O_3$	152.04722	152.04734	+	-0.80	107.04973
50	15.494	Tianshic acid	$C_{18}H_{34}O_5$	330.24165	330.24062	-	3.12	311.22437,293.21481,229.14499,171.10262
51	15.913	Umbelliferone	$C_{10}H_{10}O_2$	162.06851	162.06808	+	2.68	135.08086,133.06531,105.07056,107.08617
52	17.061	2-Desoxy-4-epipulchellin	$C_{15}H_{22}O_3$	250.15769	250.15689	+	3.17	233.15421,205.15935
53	23.367	Nervolan B	$C_{16}H_{20}O_5$	292.13221	292.13107	+	3.88	255.10027,161.06078
54	23.739	Archin	$C_{15}H_{10}O_5$	270.05391	270.05282	-	4.01	241.05156,225.05637
55	25.802	Nootkatone	$C_{15}H_{22}O$	218.16789	218.16707	+	3.87	201.16437,135.12758,109.10180
56	25.802	Zerumbone	$C_{15}H_{22}O$	218.16791	218.16707	+	3.87	201.16402
57	26.154	alantolactone	$C_{15}H_{20}O_2$	232.14710	232.10994	+	2.81	215.14403,187.14893,163.07599
58	27.033	α-Eleostearic acid	$C_{18}H_{30}O_2$	278.22546	278.22458	+	3.17	243.21107
59	28.234	Caryophyllene Oxide	$C_{15}H_{24}O$	220.18353	220.18272	+	3.68	177.1646
60	10.220	3-caffeoyl-5-feruloyquinic acid	$C_{26}H_{25}O_{12}$	530.14424	530.14243	-	3.40	353.08908,179.03502
61	11.380	CQL-hexoside	$C_{16}H_{15}O_8$	498.11700	498.11755	-	0.31	335.07852,179.03502,161.02422,135.04477
62	12.451	Tomentosin	$C_{15}H_{20}O_3$	248.14203	248.14124	+	3.15	231.13846,177.12784,135.08073
63	14.352	Parthenium	$C_{15}H_{20}O_3$	248.14208	248.14124	+	3.37	231.13884,185.13318
64	16.422	Parthenolide	$C_{14}H_{20}O_3$	248.14208	248.14124	+	3.35	231.13869,185.13306
65	22.263	Germacrone	$C_{15}H_{22}O$	218.16789	218.09677	+	-4.48	201.16443,159.11749,145.10170,121.10186,95.08630
66	22.305	Spathulenol	$C_{15}H_{24}O$	220.18347	220.18272	+	3.44	203.18019,147.11734,105.07055
67	22.431	Thymol	$C_{10}H_{14}O$	150.10497	150.10447	+	3.35	109.06561,91.05502,65.03944
68	23.448	9,10-dihydroxy-12Z-octadecenoic acid	$C_{18}H_{34}O_4$	314.24696	314.24571	-	3.97	295.22946,277.21826
69	27.980	2,4-Dimethylbenzaldehyde	$C_9H_{10}O$	134.11019	134.07316	+	3.30	107.08621
70	29.201	Dibutyl phthalate	$C_{16}H_{22}O_4$	278.15261	278.22458	+	4.09	149.02359
71	30.920	trans-Anethole	$C_{10}H_{12}O$	148.08930	148.08881	+	3.25	121.06541,107.04972,95.04996
72	41.281	Stigmasterol	$C_{29}H_{48}O$	412.37200	412.37052	+	3.59	395.36740,109.10165

Table 2. UHPLC-Q-Orbitrap HRMS data of the identified component of Heigen absorbed in serum.

NO.	RT[min]	Formula	Identification	Reference Ion	MS/MS Fragment Ions	Theoretical Mass m/z	Experimental Mass m/z	Error(ppm)
M1	33.978	$C_{10}H_{10}O_3$	coniferyl aldehyde	[M+H]+	161.06018,133.06529,118.04193	178.06362	178.06299	2.61
M2	8.587	$C_{25}H_{24}O_{12}$	Isochlorogenic acid C	[M-H]-	353.08920,173.04555,191.05620	516.12892	516.12678	4.15
M3	5.994	$C_7H_6O_4$	Protocatechuic acid	[M-H]-	135.00848,109.02900	154.02651	154.02661	-0.49
M4	9.503	$C_7H_6O_3$	4-Hydroxybenzoic acid	[M-H]-	93.03397	138.03149	138.03169	-1.46
M5	31.820	$C_{10}H_{12}O$	trans-Anethole	[M+H]+	121.06548,93.03429	148.08911	148.08881	2.01
M6	13.155	$C_9H_6O_3$	Umbelliferone	[M+H]+	135.04454,107.04970,95.04992	162.03214	162.03169	2.75
M7	10.795	$C_{10}H_{12}O_3$	Caffeic acid	[M-H]-	135.08118,107.04958	180.07889	180.07864	0.71
M8	2.821	$C_{10}H_{10}O_4$	Ferulic acid	[M+H]+	177.05440,163.03911	194.11615	194.11542	3.73
M9	12.498	$C_{16}H_{18}O_9$	Chlorogenic acid	[M-H]-	353.03174,191.05611	354.13291	354.13147	4.09
M10	21.122	$C_{16}H_{22}O_4$	Dibutyl phthalate	[M+H]+	167.03445,149.02383	278.17135	278.17044	3.1
M11	13.106	$C_8H_8O_3$	DL-Mandelic acid	[M-H]-	107.04973	152.04722	152.04734	-0.8
M12	23.841	$C_{18}H_{34}O_4$	9,10-dihydroxy-12Z-octadecenoic acid	[M-H]-	295.22772,277.21777	314.24696	314.24571	4.6
M13	36.290	$C_9H_{10}O$	2,4-Dimethylbenzaldehyde	[M+H]+	107.08611	134.07363	134.07316	3.48
M14	8.806	$C_{10}H_9O_7S$	Sulphation of FQA	[M-H]-	193.0874	274.05244	274.05238	0.22
M15	12.584	$C_9H_8O_7S$	Sulphation of CA	[M-H]-	179.10785	260.07280	260.07184	3.67
M16	7.550	$C_9H_{10}O_7S$	Sulphation of DHCA	[M-H]-	181.08719,163.07668	262.05223	262.05111	4.28
M17	6.387	$C_{18}H_{21}O_{10}$	Hydrogenation and methylation products of FQA	[M-H]-	187.00728,107.04974	398.01210	398.01032	4.46
M18	5.794	$C_{10}H_{12}O_4$	Reduction of ferulic acid	[M-H]-	151.07626,136.05229	196.07399	196.07356	2.19
M19	23.461	$C_{17}H_{20}O_{10}$	Hydroxylation products of the FQA	[M-H]-	383.07855,191.03502	384.08604	384.08452	3.97
M20	41.035	$C_{21}H_{26}O_{14}$	Decarbonylation and glucuronide conjugation of CQA	[M-H]-	325.21814	502.34666	502.34470	3.92
M21	32.342	$C_{16}H_{20}O_9$	Reduction products of CQA	[M-H]-	193.08746, 179.10779, 163.11276	356.23659	356.23514	4.05
M22	41.961	$C_{25}H_{24}O_{12}$	Glycosides of CQA	[M-H]-	339.23369,163.11267	516.36172	516.36035	2.67

compounds and 9 quinic acid metabolites were identified from mouse serum samples of Heigen.

Caffeoylquinic acid analogues mainly use m/z 179([CA-H]⁻), m/z 135 ([CA-H-CO₂]⁻) and m/z 191[QA-H]⁻, m/z 173[QA-H-H₂O] as the characteristic ionic fragment (Ouyang et al., 2017). M2 was identified as isochlorogenic acid C, produced the molecular ions at m/z 515.12164, additionally, m/z 353.08920 was the deprotonated molecular ions yield via the neutral loss of 162($C_9H_6O_3$) and m/z179.03503 was the second generation product ions via the neutral loss of m/z 174 ($C_7H_{10}O_5$). M21 deprotonated molecule ion at m/z 355.22937[M-H]⁻, which was 2 Da less than CQA, it was considered as the reduction products of CQA, fragmentation ion at m/z 193.08746, m/z 179.10779 and m/z 163.11276, therefore, M21 was identified as the reduction products of CQA. M20 with its deprotonated molecule ion at m/z 501.33923, which was 28 Da less than CQA, is considered a decarbonylation product of CQA. The fragments at m/z 325.21814 ($C_{14}H_{13}O_9$, [caffeic acid-H-CO+GluA]⁻), confirmed our earlier deduction. Therefore, M was recognized as decarbonylation and glucuronide conjugation of CQA. In the 7.550 min, M16 with m/z 261.04507 ($C_9H_9O_7S$) were confirmed to be sulphation products of dihydrocaffeic acid (DHCA) too.

The M14 was eluted at 8.806 min with an accurate protonated molecule ion at m/z 273.04514 ($C_{10}H_9O_7S$). 80 Da was more than ferulic acid, and the fragments of m/z 193.08740 ($C_{10}H_9O_4$, [M-H-SO3]⁻), and considering that the fragment ions m/z193, m/z 178, m/z 149, m/z 134 are characteristic of FQA, so it is indicated that was sulfation product of ferulic acid., so we identified it was sulphation of FQA. M17 was eluted at 6.387min and the deprotonated molecular ion was m/z 397.00507 ($C_{18}H_{21}O_{10}$), the mass was 30Da more than the FQA. Therefore, it was conjectured that as the hydrogenation and methylation products of FQA. M18 displayed the [M-H]- ion at m/z 195.06671 ($C_{10}H_{12}O_4$), and major ions are at

m/z 383.151.07626 ([M-COOH-H]⁻, m/z 136.05229 ([M-COOH-CH₃-H]⁻), so that was signed as the reduction metabolite of ferulic acid.M19 deprotonated molecule ions were observed at m/z 383.07877[M-H]⁻, in which the mass was 16 Da more than the FQA. The fragments at m/z 191.03502 ($C_7H_{11}O_6$, [quinic acid-H]⁻), so we indicated that were assigned as hydroxylation products of the FQA.

The metabolic pathways of quinic acids mainly include hydrolyzation, dehydroxylation, hydrogenation, and conjugation with glucuronic acid, and sulfate.

3.3 network pharmacology research

Targets of active ingredients of Heigen and RA

These substances may be metabolized to caffeic acid without detecting the prototype (Li et al., 2020), so the active ingredients include other quinic acid compounds identified in the Heigen extract, shown in Table 3.

Potential target prediction was performed using the SwissTargetPrediction database, collecting 296 targets based on active compounds of Heigen. In addition, a total of 1150 RA-related genes were collected from the database. Among 296 HG-related targets and 1150 RA-related targets, 113 overlapping targets were identified as core targets for subsequent investigations (Figure 3).

PPI network analysis

A PPI network was built by importing potential active targets into the STRING database, which contains 112 target proteins and 780 target interconnection proteins. To further analyze the protein-protein interactions, using Cytoscape (v3.9.0) software to construct a new PPI network (Figure 4). Among the

network, The CytoNCA plugin in Cytoscape software was used to mine the primary objectives. The following were the selection criteria based on triple median values: Degree≥29, Betweenness ≥236.239965, and Closeness ≥0.53370315. Finally, A core PPI network with 10 nodes and 42 edges was eliminated. In the core PPI network, the Color and shape size reflect the degree value of genes. The targets with the highest value top 10 were AKT1, PTGS2, MMP9, EGFR, CASP3, PPARG, TLR4, ESR1, CCND1, and MAPK8 which may play an important role in the RA effect of Heigen.

GO and KEGG analysis

The GO analysis concludes biological processes (BP), cellular components (CC), and molecular functions (MF). It obtained 1308 GO terms in total, including 1087 of BP, 71 of CC, and 150 of MF. The top 10 significant enrichment terms of BP, CC, and MF with the highest gene counts were visualized in a bubble diagram in Figure 4. It showed that the biological mechanisms of action of the Heigen in the treatment of RA were mainly related to the reaction of cells to hormone levels and inflammatory response. The metabolic processes of olefinic compounds and regulation of defense response were

also involved. Cell components, such as membrane raft, vesicle lumen, and GABA-A receptor complexes, were also involved in the mechanism of action of Heigen. Further, the result showed the activity of monooxygenase, oxidoreductase, endopeptidase, and serine hydrolase were related to the molecular mechanism of Heinen. The KEGG analysis (P < 0.01) revealed a total of 154 signaling pathways, which included TNF, IL-17, C-type lectin receptor, Toll-like receptor, Prolactin, and NF-kappa B signaling pathways. The results are shown in Figure 5.

Construction of "active ingredients-targeted genes-pathway" network

Construction of an 'active compound–targeted genes-pathway' network diagram (Figure 6). Each of these active molecules covered numerous targets. It is a shred of clear evidence that when Heigen is used as an anti-RA drug, multiple targets

Figure 3. Venn diagram for intersection analysis of compound targets and disease targets.

Table 3. Active compounds, their properties, and the number of disease targets.

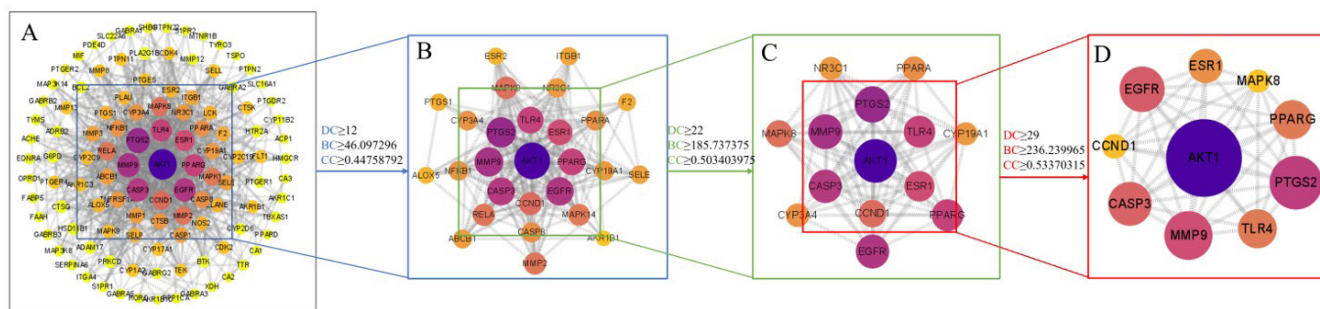| Compound	Pubchem ID	Bioavailability Score	Disease Targets
1,3- Dicaffeoylquinic acid	6474640	0.11	18
3-Feruloylquinic acid	10133609	0.11	12
4-Feruloylquinic acid	10177048	0.11	14
4-Hydroxybenzoic acid	135	0.85	3
4-Methoxycinnamic acid	699414	0.85	7
5-Feruloylquinic acid	10133609	0.11	12
9,10-dihydroxy-12Z-octadecenoic acid	9966640	0.56	47
Caffeic acid	689043	0.56	9
Chlorogenic acid	1794427	0.11	5
coniferyl aldehyde	5280536	0.55	3
Cryptochlorogenic acid	9798666	0.11	6
Dibutyl phthalate	3026	0.55	48
ferulic acid	445858	0.85	2
Isochlorogenic acid A	6474310	0.11	12
Isochlorogenic acid B	5281780	0.11	24
Isochlorogenic acid C	6474309	0.11	24
Neochlorogenic acid	5280633	0.11	5
protocatechuic acid	72	0.56	3
trans-Anethole	637563	0.55	1
Umbelliferone	5281426	0.55	20

Figure 4. Protein–protein interaction (PPI) network. A: The interactive PPI network of Heigen acting on RA putative targets. B: Target proteins screening by the median of DC, BC, CC from A. C: Screened targets genes from B. D: PPI network of 10 key target screening from C. Each ellipsis represents a Heigen and RA-related target protein. The hue of nodes is inversely related to their degrees.
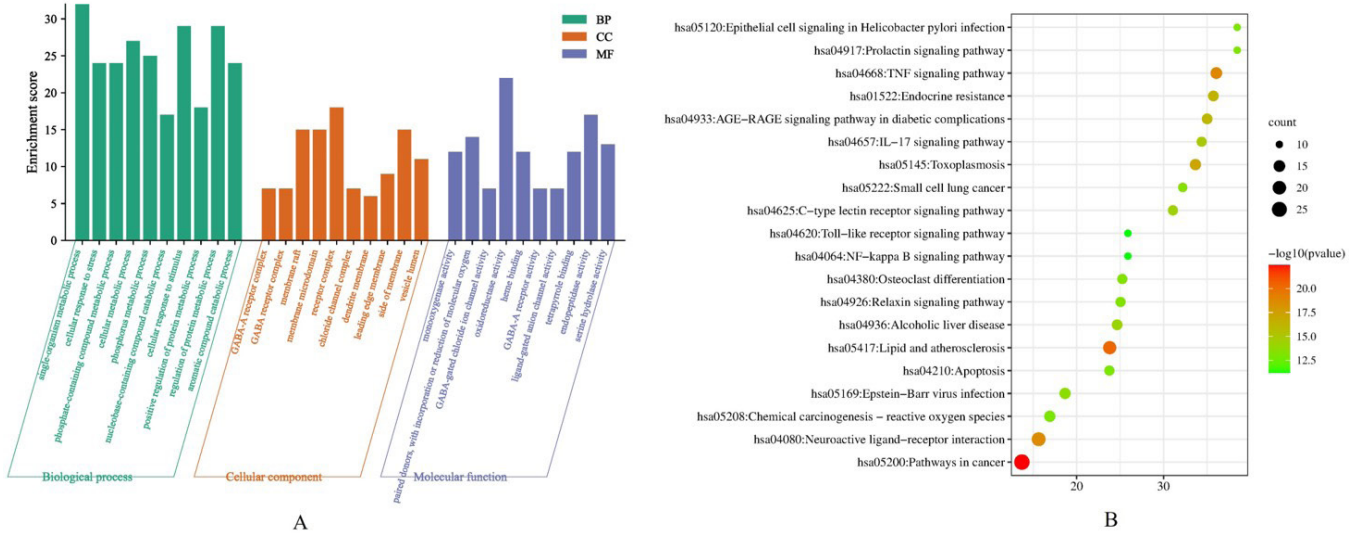
Figure 5. (A) Enrichment analyses of the potential targets of the Heigen in the treatment of RA, biological process (BP); cellular component (CC); molecular function (MF); (B) KEGG pathway analysis of target genes.
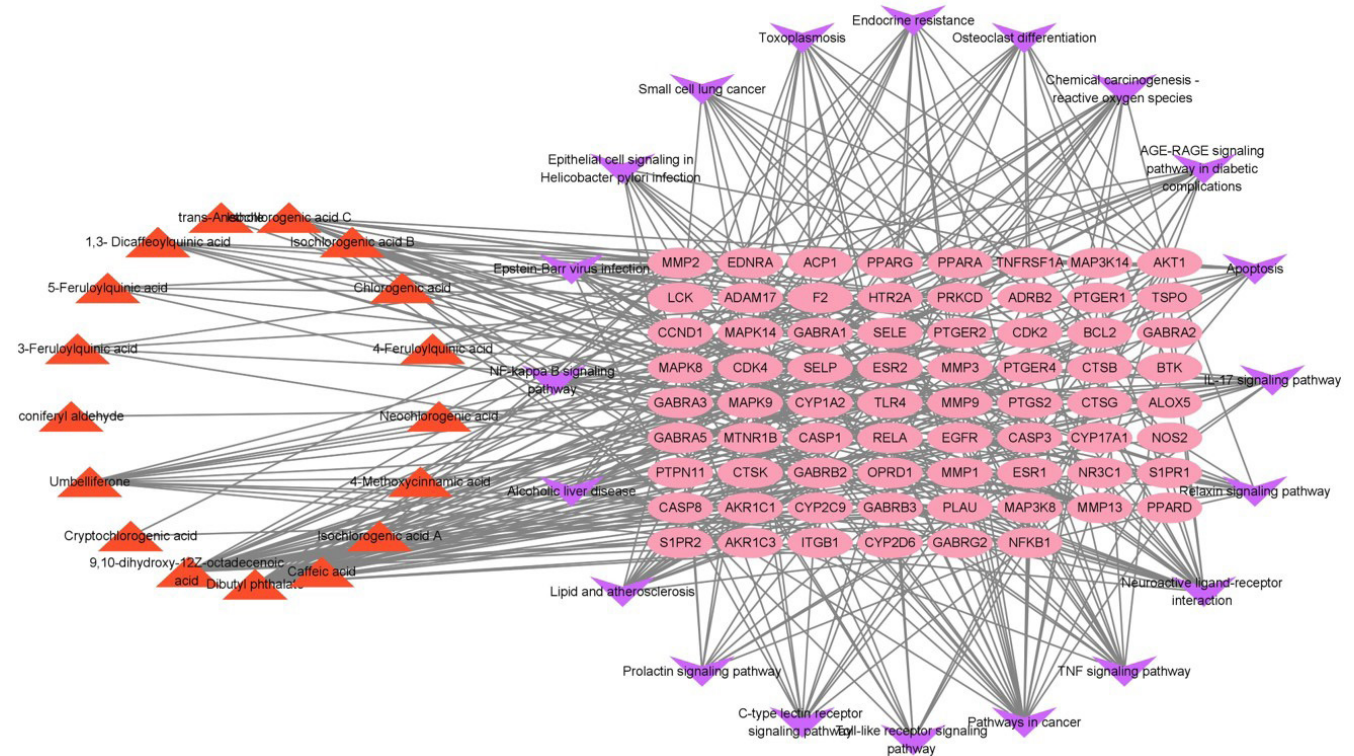

Figure 6. Pathway influenced by Heigen. The tangerine nodes represent the active compounds, the pink nodes represent the hub genes, and the purple nodes are the pathways associated with the targets.

may have synergistic activity. Based on the degree of these compounds in the compound–targeted genes-pathways network, the top 10 active compounds in degree were dibutyl phthalate, 9,10-dihydroxy-12Z-octadecenoic acid, isochlorogenic acid B, isochlorogenic acid C, umbelliferone, 1,3-Dicaffeoylquinic acid, 4-Feruloylquinic acid, caffeic acid, 3-Feruloylquinic acid, 5-Feruloylquinic, which indicate that quinic acids may be the active ingredient groups of RA in Heigen.

3.4 molecular docking verification

Dibutyl phthalate, 9,10-dihydroxy-12Z-octadecenoic acid, Isochlorogenic acid B, Isochlorogenic acid C, Umbelliferone, 1,3-Dicaffeoylquinic acid, 4-Feruloylquinic acid, Caffeic acid, 3-Feruloylquinic acid, 5-Feruloylquinic acid were identified as the top 10 active compounds in degree. These main active ingredients are related to the following genes: AKT1, PTGS2, MMP9, EGFR, CASP3, PPARG, TLR4, ESR1, CCND1, and MAPK8, the molecular docking results shown in Table 4. The compound structures download from PubChem (Lin at al., 2022). The main results are visualized by Pymol as shown

in Figure 7, these docking results indicate that these active components were bound to the target protein's active site.

4 Discussion

RA is a prevalent systemic inflammatory autoimmune disease that causes significant disability and has a high incidence, which can significantly impair physical function and quality of life (Liu et al., 2022). Recent findings have advanced our knowledge of rheumatoid arthritis and its implications. Heigen has been widely used as food and medicine since the ancient dynasty of China, particularly in the treatment of RA. However, no thorough

Table 4. Molecular docking results of the top 10 components with the top 10 target proteins.

| Ligand	Proteins									
	Affinity (kcal/mol)									
	AKT1	PTGS2	MMP9	EGFR	CASP3	PPARG	TLR4	ESR1	CCND1	MAPK8
Dibutyl phthalate	-4.7	-6.9	-4.9	-5.8	-6.0	-5.6	-6.4	-4.9	-5.6	-6.4
9,10-dihydroxy-12Z-octadecenoic acid	-4.4	-5.9	-4.9	-6.0	-6.5	-5.8	-6.3	-5.9	-5.4	-6.6
Isochlorogenic acid B	-7.5	-11.1	-8.3	-8.6	-7.7	-8.0	-9.0	-7.9	-7.2	-10.1
Isochlorogenic acid C	-6.2	-10.2	-8.3	-8.2	-8.3	-8.2	-9.5	-7.5	-6.9	-9.7
Umbelliferone	-5.4	-7.8	-6.5	-6.6	-6.2	-6.1	-6.5	-6.5	-6.4	-6.8
1,3-Dicaffeoylquinic acid	-6.2	-10.8	-7.5	-7.2	-8.7	-8.8	-7.9	-7.2	-7.7	-9.7
4-Feruloylquinic acid	-6.2	-8.6	-7.3	-6.9	-7.5	-6.6	-7.6	-6.6	-6.8	-9.1
Caffeic acid	-5.4	-6.9	-6.3	-6.8	-6	-6.1	-6.2	-6.2	-7.2	-6.5
3-Feruloylquinic acid	-6.1	-8.3	-6.5	-7.3	-8.1	-7.2	-7.6	-6.8	-6.8	-9.3
5-Feruloylquinic acid	-6.4	-8.0	-6.8	-7.4	-7.9	-7.0	-7.4	-8	-6.6	-9.2
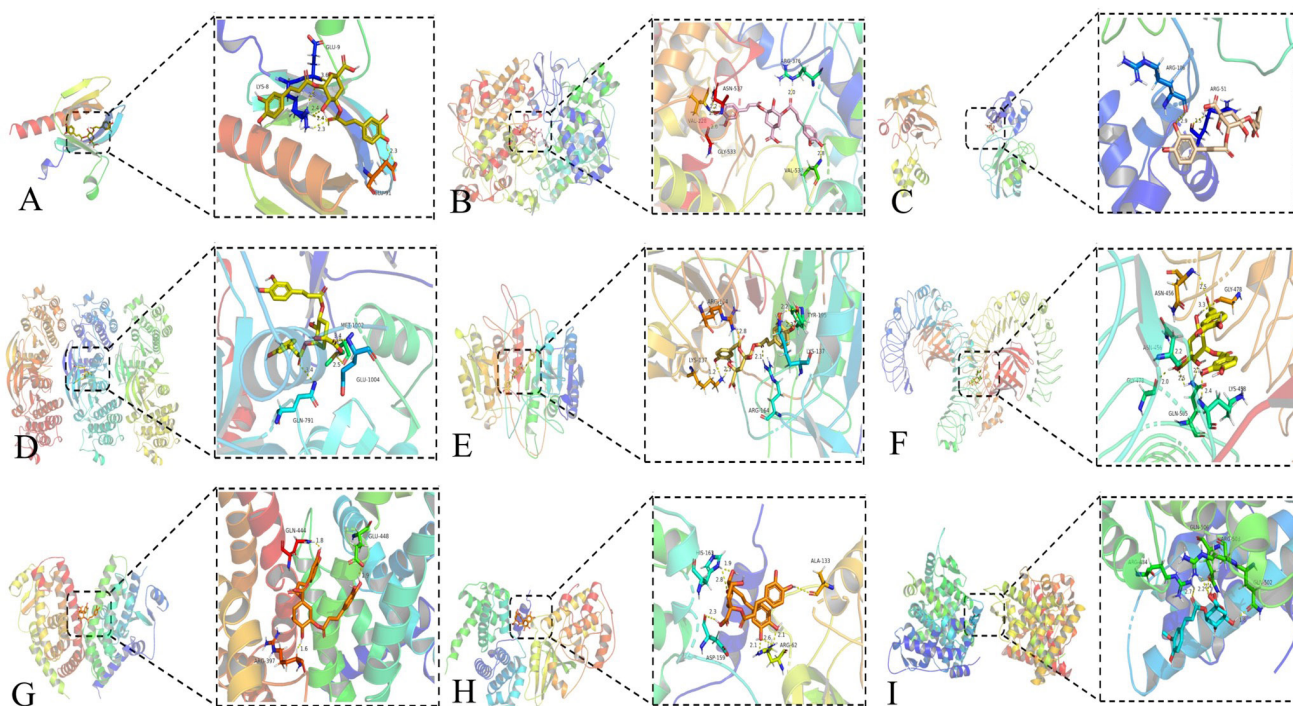
Figure 7. Molecular docking of active compounds of Heigen and receptor protein. (A-D). ischlorogenic acid B with AKT1, PTGS2, MMP9, EGFR protein; (E-F). Isochlorogenic acid C with CASP3, TLR4 protein; (G-H). 1,3-Dicaffeoylquinic acid with PPARG, CCND1 protein; (I) 5-Feruloylquinic acid with ESR1 protein.

examination of its material basis, targets, and mechanisms of action has been performed so far. In this study, we analyzed the active ingredients and mechanisms of action of Heigen in the treatment of RA based on UHPLC-Q-Orbitrap HRMS and different databases, combined with network pharmacology analysis and molecular docking.

According to the active ingredient target network diagram, dibutyl phthalate, 9,10-dihydroxy-12Z-octadecenoic acid, Isochlorogenic acid B, Isochlorogenic acid C, Umbelliferone, 1,3-Dicaffeoylquinic acid, 4-Feruloylquinic acid, Caffeic acid, 3-Feruloylquinic acid, 5-Feruloylquinic acid showed as the most potent active components of Heigen. There is accumulating evidence that ICGA exerts several biological activities, such as antioxidant, and anti-inflammatory (Upadhyay, 2016). Previous studies have shown that caffeic acid can induce cell apoptosis in RA-FLS and reduce productions of IL-6 and TNF-α in FLS (Wang et al., 2017), and it as caspase inhibitors have been regarded as an effective strategy for attenuation of cartilage erosion (Fikry et al., 2019). Related studies show that umbelliferone can modulate the antioxidant enzymes and suppress NF-kB production and can inhibit the TNFα, IL-6, and IL-1β, which indicates that umbelliferone reduction osteoclast differentiation by CFA-induced model (Wu et al., 2021).

The PPI interaction analysis showed that the main targets included AKT1, PTGS2, MMP9, EGFR, CASP3, PPARG, TLR4, ESR1, CCND1, and MAPK8. Among these targets, AKT1 is one of 3 closely related serine/threonine-protein kinases called the AKT kinase, which controls several activities such as metabolism, proliferation, cell survival, growth, and angiogenesis (Liu et al., 2021b). PTGS2 (Prostaglandin-Endoperoxide Synthase 2) is a protein coding gene, which is expressed in cells of COX-1 and COX-2, and played a particular role in the inflammatory response (Shen et al., 2022). CASP3 plays a central role in the execution phase of cell apoptosis, involving the signaling pathways of apoptosis, necrosis, and inflammation (Zhang et al., 2019). MMP9 is abundant in synovial and subchondral bone-infiltrating inflammatory cells, pannuclear tissues, and multinucleated cells, including osteoclasts, it is involved in joint destruction, cytokine and chemokine activation, and tissue destruction through basement membrane degradation of the epithelium and vasculature (Takai & Jin, 2022).

According to the KEGG pathway analysis, multiple inflammation-related and apoptosis signaling pathways are highly relevant to RA, such as TNF signaling pathways, IL-17 signaling pathways, and NF-κB signaling pathways are the main therapeutic pathways involved in the Heigen way of action. The levels of IL-17 are significantly increased in the synovial fluid of RA patients, which can promote RANKL expression to stimulate synovial inflammation, angiogenesis, and osteoclast formation (Yang et al., 2019). Furthermore, the secretion of IL-17 can further activate the corresponding receptor to recruit ACT1,then activate NF-κB signaling pathways by initiating TNF receptor-associated factor 6 (TRAF6) which can activethe various immune cells including macrophages (Wang et al., 2022) mast cells, neutrophils, and B cells (Bystrom et al., 2018). TNF is an important cytokine that induces various intracellular signaling pathways such as apoptosis, cell survival, inflammation, and immunity (Webster & Vucic, 2020), it can repress osteoblast differentiation and bone formation by activating the NF-κB signaling pathway. These

studies improved RA Heigen's predictions of inflammation associated with this pathway. However, It is required to validate them with a more experimental investigation.

Finally, we assessed the binding strength of the parent drug to the target protein using molecular docking. The binding energy was routinely measured to assess the degree of affinity of components with targets. It is generally accepted that binding energy which is less than 0 kcal/mol indicates that the ligand and the receptor spontaneously combined (Liu et al., 2021a). The main compounds in Heigen were identified to blind to core target proteins confirmed by molecular docking.

The obtained findings provided strong theoretical evidence for the use of Heigen in the treatment of RA. Firstly, we used the method of UHPLC-Q-Orbitrap HRMS to identify the total number of chemical constituents of Heigen and the metabolites of the rat serum. Secondly, we obtained the bioactive compounds by the method of network pharmacology and molecular docking, and found the mechanisms in the treatment of RA is mainly by acting on multiple inflammatory pathways.

The result is to establish a theoretical foundation for fully using Heigen medicinal material resources, as well as to create the groundwork for development and utilization of food of the same origin as medicine and food. Heigen can be further developed as a source of functional food ingredients or dietary supplements to relieve RA. Nevertheless, the core compounds, hub targets, and related pathways were predicted by computational tools, but it still needs further verification to validate the molecular mechanism of Heigen for the treatment of RA.

5 Conclusions

It is complicated to comprehend the treatment mechanisms of TCM because of the complexity of the substances, unknown targets, and underlying systems. In this study, using UHPLC-Q-Orbitrap HRMS, it was identified 72 components and 22 metabolites. Then, integrated serum pharmacochemistry with network pharmacology and docking analysis to identify the potential active components of Heigen and predicted the functional mechanisms of Heigen in anti-RA. This provides a scientific reference for the research and application of Heigen, as well as a referable foundation for studying the mechanism of Heigen in the treatment of rheumatoid arthritis.

Declaration of competing interest

The authors declare that there are no competing financial interests in this paper.

Acknowledgements

References

Alamgeer, H., Hasan, U. H., Uttra, A. M., Qasim, S., Ikram, J., Saleem, M., & Niazi, Z. R. (2020). Phytochemicals targeting matrix

metalloproteinases regulating tissue degradation in inflammation and rheumatoid arthritis. *Phytomedicine*, 66, 153134. http://dx.doi.org/10.1016/j.phymed.2019.153134. PMid:31812101.

Bindu, S., Mazumder, S., & Bandyopadhyay, U. (2020). Non-steroidal anti-inflammatory drugs (NSAIDs) and organ damage: a current perspective. *Biochemical Pharmacology*, 180, 114147. http://dx.doi.org/10.1016/j.bcp.2020.114147. PMid:32653589.

Bystrom, J., Clanchy, F. I., Taher, T. E., Mangat, P., Jawad, A. S., Williams, R. O., & Mageed, R. A. (2018). TNFα in the regulation of Treg and Th17 cells in rheumatoid arthritis and other autoimmune inflammatory diseases. *Cytokine*, 101, 4-13. http://dx.doi.org/10.1016/j.cyto.2016.09.001. PMid:27639923.

Cheng, X.-R., Ma, J.-H., Amadou, I., Zhao, W., Chen, Y.-Y., Zhang, C.-X., & Guan, B. (2023). Electrophilic components from Xiaoheiyao (rhizomes of Inula nervosa Wall.) alleviate the production of heterocyclic aromatic amines via creatinine inhibition. *Food Chemistry*, 404(Pt A), 134561. http://dx.doi.org/10.1016/j.foodchem.2022.134561. PMid:36252379.

Dias, I. R. S. R., Lo, H. H., Zhang, K., Law, B. Y. K., Nasim, A. A., Chung, S. K., Wong, V. K. W., & Liu, L. (2021). Potential therapeutic compounds from traditional Chinese medicine targeting endoplasmic reticulum stress to alleviate rheumatoid arthritis. *Pharmacological Research*, 170, 105696. http://dx.doi.org/10.1016/j.phrs.2021.105696. PMid:34052360.

Fikry, E. M., Gad, A. M., Eid, A. H., & Arab, H. H. (2019). Caffeic acid and ellagic acid ameliorate adjuvant-induced arthritis in rats via targeting inflammatory signals, chitinase-3-like protein-1 and angiogenesis. *Biomedicine and Pharmacotherapy*, 110, 878-886. http://dx.doi.org/10.1016/j.biopha.2018.12.041. PMid:30562713.

Fonseca Peixoto, R., Ewerton Maia Rodrigues, C., Henrique de Sousa Palmeira, P., Cézar Comberlang Queiroz Davis dos Santos, F., Keesen de Souza Lima, T., & de Sousa Braz, A. (2022). Immune hallmarks of rheumatoid arthritis management: a brief review. *Cytokine*, 158, 156007. http://dx.doi.org/10.1016/j.cyto.2022.156007. PMid:35985174.

Ghane, M., Babaeekhou, L., & Shams, M. (2022). Antimicrobial activity of Rhus Coriaria L. and Salvia Urmiensis bunge against some food-borne pathogens and identification of active components using molecular networking and docking analyses. *Food Science and Technology (Campinas)*, 42, e08221. http://dx.doi.org/10.1590/fst.08221.

Hu, Y., Liu, S., Liu, W., Zhang, Z., Liu, Y., Li, S., Sun, D., Zhang, G., & Fang, J. (2022). Potential molecular mechanism of yishen capsule in the treatment of diabetic nephropathy based on network pharmacology and molecular docking. *Diabetes, Metabolic Syndrome and Obesity*, 15, 943-962. http://dx.doi.org/10.2147/DMSO.S350062. PMid:35378831

Jian, L., Guo, J., Zhang, Y., Liu, J., Liu, Y., & Xu, J. (2022). Using integrated GC-MS analysis, in vitro experiments, network pharmacology: exploring migao fatty oil active components/mechanisms against coronary heart disease. *Food Science and Technology (Campinas)*, 42, e89322. http://dx.doi.org/10.1590/fst.89322.

Lee, W.-Y., Lee, C.-Y., Kim, Y.-S., & Kim, C.-E. (2019). The methodological trends of traditional herbal medicine employing network pharmacology. *Biomolecules*, 9(8), E362. http://dx.doi.org/10.3390/biom9080362. PMid:31412658.

Li, R.-L., Duan, H.-X., Liang, Q., Huang, Y.-L., Wang, L.-Y., Zhang, Q., Wu, C.-J., Liu, S.-Q., & Peng, W. (2022). Targeting matrix metalloproteases: a promising strategy for herbal medicines to treat rheumatoid arthritis. *Frontiers in Immunology*, 13, 1046810. http://dx.doi.org/10.3389/fimmu.2022.1046810. PMid:36439173.

Li, Z., Chen, J., Gao, X., Zhang, T., Zheng, W., Wei, G., Huang, Y., Qi, J., Zhang, Y., & Ma, P. (2020). Identification of components and

metabolites in plasma of type 2 diabetic rat after oral administration of Jiao-Tai-Wan using ultra-performance liquid chromatography/quadrupole time-of-flight mass spectrometry. *Journal of Separation Science*, 43(13), 2690-2707. http://dx.doi.org/10.1002/jssc.201901040. PMid:32246812.

Lin, J., Gu, J., Fan, D., & Li, W. (2022). Herbal formula modified bu-shen-huo-xue decoction attenuates intervertebral disc degeneration via regulating inflammation and oxidative stress. *Evidence-Based Complementary and Alternative Medicine: ECAM*, 2022, 4284893. http://dx.doi.org/10.1155/2022/4284893. PMid:35154344.

Liu, C., Fan, F., Zhong, L., Su, J., Zhang, Y., & Tu, Y. (2022). Elucidating the material basis and potential mechanisms of Ershiwuwei Lvxue Pill acting on rheumatoid arthritis by UPLC-Q-TOF/MS and network pharmacology. *PLoS One*, 17(2), e0262469. http://dx.doi.org/10.1371/journal.pone.0262469. PMid:35130279.

Liu, J., Liu, J., Tong, X., Peng, W., Wei, S., Sun, T., Wang, Y., Zhang, B., & Li, W. (2021a). Network pharmacology prediction and molecular docking-based strategy to discover the potential pharmacological mechanism of huai hua san against ulcerative colitis. *Drug Design, Development and Therapy*, 15, 3255-3276. http://dx.doi.org/10.2147/DDDT.S319786. PMid:34349502.

Liu, J.-Q., Liu, J., Tong, X.-L., Peng, W.-J., Wei, S.-S., Sun, T., Wang, Y.-K., Zhang, B.-K., & Li, W.-Q. (2021). Network Pharmacology Prediction and Molecular Docking-Based Strategy to Discover the Potential Pharmacological Mechanism of Huai Hua San Against Ulcerative Colitis. *Drug Design, Development and Therapy*, 15, 3255-3276. http://dx.doi.org/10.2147/DDDT.S319786.

Liu, S., Ma, H., Zhang, H., Deng, C., & Xin, P. (2021b). Recent advances on signaling pathways and their inhibitors in rheumatoid arthritis. *Clinical Immunology (Orlando, Fla.)*, 230, 108793. http://dx.doi.org/10.1016/j.clim.2021.108793. PMid:34242749.

Min, H. K., Kim, S. H., Kim, H.-R., & Lee, S.-H. (2022). Therapeutic Utility and adverse effects of biologic disease-modifying anti-rheumatic drugs in inflammatory arthritis. *International Journal of Molecular Sciences*, 23(22), 13913. http://dx.doi.org/10.3390/ijms232213913. PMid:36430392.

Ouyang, H., Li, J., Wu, B., Zhang, X., Li, Y., Yang, S., He, M., & Feng, Y. (2017). A robust platform based on ultra-high performance liquid chromatography Quadrupole time of flight tandem mass spectrometry with a two-step data mining strategy in the investigation, classification, and identification of chlorogenic acids in Ainsliaea fragrans Champ. *Journal of Chromatography. A*, 1502, 38-50. http://dx.doi.org/10.1016/j.chroma.2017.04.051.

Shen, Y., Teng, L., Qu, Y., Liu, J., Zhu, X., Chen, S., Yang, L., Huang, Y., Song, Q., & Fu, Q. (2022). Anti-proliferation and anti-inflammation effects of corilagin in rheumatoid arthritis by downregulating NF-κB and MAPK signaling pathways. *Journal of Ethnopharmacology*, 284, 114791. http://dx.doi.org/10.1016/j.jep.2021.114791. PMid:34737112.

Smolen, J. S., Aletaha, D., & McInnes, I. B. (2016). Rheumatoid arthritis. *Lancet*, 388(10055), 2023-2038. http://dx.doi.org/10.1016/S0140-6736(16)30173-8. PMid:27156434.

Takai, S., & Jin, D. (2022). Pathophysiological Role of Chymase-Activated Matrix Metalloproteinase-9. *Biomedicines*, 10(10), 10. http://dx.doi.org/10.3390/biomedicines10102499. PMid:36289761.

Upadhyay, R. K. (2016). Anti-arthritic potential of plant natural products; its use in joint pain medications and anti-inflammatory drug formulations. *International Journal of Green Pharmacy*, 10(3), 3. http://dx.doi.org/10.22377/ijgp.v10i3.698.

Wang, N., Xu, C., Li, N., Wang, F., Wang, F., Li, Z., Yu, Q., & Zhang, G. (2022). Synergistic anti-inflammatory effects of resveratrol and vitamin E in lipopolysaccharide-induced RAW264.7 cells. *Food*

Science and Technology (Campinas), 42, e24122. http://dx.doi.org/10.1590/fst.24122.

Wang, W., Sun, W., & Jin, L. (2017). Caffeic acid alleviates inflammatory response in rheumatoid arthritis fibroblast-like synoviocytes by inhibiting phosphorylation of IκB kinase α/β and IκBα. *International Immunopharmacology*, 48, 61-66. http://dx.doi.org/10.1016/j.intimp.2017.04.025. PMid:28463788.

Wang, Y., Xue, B., Wang, X., Wang, Q., Liu, E., & Chen, X. (2021). Pharmacokinetic study of Tangwang Mingmu granule for the management of diabetic retinopathy based on network pharmacology. *Pharmaceutical Biology*, 59(1), 1334-1350. http://dx.doi.org/10.1080/13880209.2021.1979051. PMid:34590544.

Webster, J. D., & Vucic, D. (2020). The balance of TNF mediated pathways regulates inflammatory cell death signaling in healthy and diseased tissues. *Frontiers in Cell and Developmental Biology*, 8, 365. http://dx.doi.org/10.3389/fcell.2020.00365. PMid:32671059.

Wu, G., Nie, W., Wang, Q., Hao, Y., Gong, S., Zheng, Y., & Lv, H. (2021). Umbelliferone ameliorates complete freund adjuvant–induced arthritis via reduction of NF-κB signaling pathway in osteoclast differentiation. *Inflammation*, 44(4), 1315-1329. http://dx.doi.org/10.1007/s10753-021-01418-x. PMid:33484396.

Yang, J., Tang, C.-T., Jin, R.-R., Liu, B.-X., Wang, P., Chen, Y.-X., & Zeng, C.-Y. (2022). Molecular mechanisms of Huanglian jiedu decoction on ulcerative colitis based on network pharmacology and molecular docking. *Scientific Reports*, 12(1), 1-15. http://dx.doi.org/10.1038/s41598-022-09559-1.

Yang, P., Qian, F.-Y., Zhang, M.-F., Xu, A.-L., Wang, X., Jiang, B.-P., & Zhou, L.-L. (2019). Th17 cell pathogenicity and plasticity in rheumatoid arthritis. *Journal of Leukocyte Biology*, 106(6), 1233-1240. http://dx.doi.org/10.1002/JLB.4RU0619-197R. PMid:31497905.

Yin, F., Zhou, X., Kang, S., Li, X., Li, J., Ullah, I., Zhang, A., Sun, H., & Wang, X. (2022). Prediction of the mechanism of Dachengqi Decoction treating colorectal cancer based on the analysis method of " into serum components -action target-key pathway. *Journal of Ethnopharmacology*, 293, 115286. http://dx.doi.org/10.1016/j.jep.2022.115286.

Zhang, Q., Liu, J., Zhang, M., Wei, S., Li, R., Gao, Y., Peng, W., & Wu, C. (2019). Apoptosis Induction of fibroblast-like synoviocytes is an important molecular-mechanism for herbal medicine along with its active components in treating rheumatoid arthritis. *Biomolecules*, 9(12), 795. http://dx.doi.org/10.3390/biom9120795. PMid:31795133.

Zhang, W., Tian, W., Wang, Y., Jin, X., Guo, H., Wang, Y., Tang, Y., & Yao, X. (2022). Explore the mechanism and substance basis of Mahuang FuziXixin Decoction for the treatment of lung cancer based on network pharmacology and molecular docking. *Computers in Biology and Medicine*, 151(Pt A), 106293. http://dx.doi.org/10.1016/j.compbiomed.2022.106293.

Zhao, X., Liu, J., Yang, L., Niu, Y., Ren, R., Su, C., Wang, Y., Chen, J., & Ma, X. (2021). Beneficial effects of mijianchangpu decoction on ischemic stroke through components accessing to the brain based on network pharmacology. *Journal of Ethnopharmacology*, 285, 114882. http://dx.doi.org/10.1016/j.jep.2021.114882.